The Advection Boundary Law in presence of mean-flow and spinning modes

Emanuele de Bono, Manuel Collet, Morvan Ouisse, Edouard Salze, Maxime Volery, Hervé Lissek, Jacky Mardjono

The Advection Boundary Law in presence of mean-flow and spinning modes

Emanuele De Bono [1], **Manuel Collet** [1]
[1] Ecole Centrale de Lyon, CNRS, ENTPE, LTDS, UMR5513, 69130 Ecully, France
emanuele.de-bono@ec-lyon.fr

Morvan Ouisse [2],
[2] SUPMICROTECH, Université de Franche-Comté, CNRS, institut FEMTO-ST, F-25000 Besançon, France.
Edouard Salze [3]
[3] Ecole Centrale de Lyon, LMFA, 69130 Écully, France.
Maxime Volery [4], **Hervé Lissek** [4]
[4] Signal Processing Laboratory LTS2,
École Polytechnique Fédérale de Lausanne, Station 11, CH-1015 Lausanne, Switzerland.
Jacky Mardjono [5]
[5] Safran Aircraft Engines, F-75015, Paris, France.

May 29, 2024

Abstract

In the attempt to reduce fuel consumption, a new generation of Ultra-High-By-Pass-Ratio (UHBR) turbofans have been introduced in the aeronautic industry which are structurally noisier especially at lower frequencies, because of their larger diameter, lower number of blades and rotational speed. Moreover, they present a shorter nacelle, leaving less available space for acoustic treatments. For this reason, innovation in the liner technology is highly demanded. In this contribution, we analyse the performances of an electroacoustic liner, made up of microphones (sensors) and small loudspeakers (actuators). Such array of electroacoustic resonators can feature an interesting boundary operator, called Advection Boundary Law. Such boundary law has been analysed in grazing-incident acoustic fields without air-flow and in case of plane waves. Here, we adapt such boundary condition to

Figure 1: Illustration of the scattering problem in acoustic waveguide, with guided modes amplitudes definition on the left side, and on the right side of the acoustically treated segment.

attenuate spinning modes. Numerical simulations in case of spinning-modes, shows the potentiality and the passivity issues of such innovative boundary law. Finally, a reproduction of a turbofan engine (scale 1:3) accomplishing real-life rotational speeds, allows to assess the performances of the Advection Boundary Law in presence of mean-flow and spinning-modes.

1 INTRODUCTION

The industrial contest is the noise transmission control in turbofan aircraft engines, where higher performances are demanded to the acoustic liners by the UHBR turbofan technologies. In order to overcome the limitations of classical liners, the Salute project designed an electroacoustic liner made up of Electroacoustic Resonators (ER) [1, 2, 3, 4, 5, 6]. Four collocated microphones and a speaker allow to implement generalized impedances, also involving the first spatial derivatives of sound pressure on the boundary. In this contribution, we study a non-local control law, called Advection Boundary Law (ABL). In Section 1.1, we present the scattering simulations on a cylindrical waveguide excited by spinning modes. Then, in Section 2, we present the attenuation of the azimuthal modes achieved on the Phare2 test-bench [7, 8], confirming the potentiality of such innovative liner.

1.1 Multi-modal scattering

In this section, we aim at solving the multi-modal scattering problem in case of absence of mean-flow. It is defined as in Eq. (1), where the terms C_μ^+, A_γ^-, A_ν^+ and C_σ^- are illustrated in Figure 1. The transmission coefficient matrix for example, $[T_{\mu,\nu}^+]$, links the amplitudes of the incident guided modes $\{A_\nu^+\}$ (with varying mode index "ν") to the amplitudes of the transmitted guided modes $\{C_\mu^+\}$ (of varying index "μ").

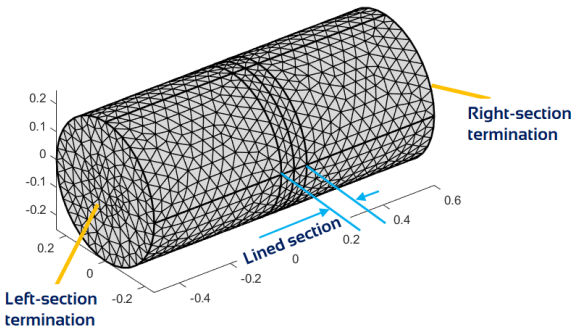

Figure 2: Mesh of the cylinder FE model, with the treated (lined) segment specified, as well as the right and left terminations.

$$\begin{bmatrix} \{C_\mu^+\} \\ \{A_\gamma^-\} \end{bmatrix} = \begin{bmatrix} [\boldsymbol{T}_{\boldsymbol{\mu},\boldsymbol{\nu}}^+] & [\boldsymbol{R}_{\boldsymbol{\mu},\boldsymbol{\sigma}}^-] \\ [\boldsymbol{R}_{\boldsymbol{\gamma},\boldsymbol{\nu}}^+] & [\boldsymbol{T}_{\boldsymbol{\gamma},\boldsymbol{\sigma}}^-] \end{bmatrix} \begin{bmatrix} \{A_\nu^+\} \\ \{C_\sigma^-\} \end{bmatrix} \tag{1}$$

In COMSOL Multiphysics, a Finite-Element (FE) model of a cylinder of radius 0.25 m, with a treated segment of 0.1 m, has been created, see Figure 2. The segments on the left and on the right side of the treated segment has been defined sufficiently far from the respective terminations in order to avoid border effects.
In order to define indicators for the transmission, reflection and absorption performances of the liner, the acoustic intensity has to be defined:

$$I(\omega, x) = \frac{1}{2} \int_0^R \int_0^{2\pi} \mathrm{Re}\{p(x, r, \theta, \omega)\ v^*(x, r, \theta, \omega)\} r dr d\theta, \tag{2}$$

where th superscript * indicates the complex conjugate. The acoustic intensities can be computed at the left and right terminations, by exploiting the orthogonality condition between guided modes in rigid waveguides. Supposing to excite the system by incident modes $A_\nu^+(\omega) \neq 0$ and $C_\sigma^-(\omega) = 0$, the pressure $p^L(\omega)$ at the left section, can be written in terms of the reflection coefficients $R_{\gamma,\nu}^+(\omega)$ as in Eq. (3a). The acoustic velocity $v^L(\omega)$ along the longitudinal direction, is easily retrieved in Eq. (3b) from the Euler equation along the longitudinal direction x: $-\rho_0 \partial_t v_x = \partial_x p$.

$$p_L(\omega) = \sum_\nu A_\nu^+(\omega) \sum_\gamma J_{m(\gamma)}(k_{r_{m(\gamma)n(\gamma)}} r) e^{\mathrm{j}m(\gamma)\theta} \Big(\delta_{\nu,\gamma} + R_{\gamma,\nu}^+(\omega) \Big), \tag{3a}$$

$$v_L(\omega) = \frac{1}{\rho_0 \mathrm{j}\omega} \sum_{\nu} (A_\nu^+(\omega))^* \sum_{\gamma} J^*_{m(\gamma)}(k_{r_{m(\gamma)n(\gamma)}} r) e^{-\mathrm{j}m(\gamma)\theta} \left(\mathrm{j}k^*_{x_\nu}(\omega)\delta_{\nu,\gamma} - \mathrm{j}k^*_{x_\gamma}(\omega)(R^+_{\gamma,\nu}(\omega))^* \right), \tag{3b}$$

From Eq. (2), and by choosing the opportune normalization of the Bessel function mode-shapes $J_{m(\gamma)}$, the acoustic intensity at the left-section termination $I_L(\omega)$ expression of Eq. (4a) is obtained [9]. Analogously, the acoustic intensity $I_R(\omega)$ can be evaluated at the right termination in terms of the transmission coefficient $T^+_{\mu,\nu}(\omega)$ as in Eq. (4b). Observe that in Eq.s (4), we assume to neglect the so-called *tunnelling effect* [9], which is an acceptable assumption as long as the computation is performed sufficiently far from duct discontinuities, so that to discard contribution of evanescent modes.

$$I_L(\omega) = \frac{\pi R}{\rho_0 \omega} \sum_{\nu} |A^+_\nu(\omega)|^2 \sum_{\gamma} \left(\mathrm{Re}\{k_{x_\nu}(\omega)\}\delta_{\nu,\gamma} - \mathrm{Re}\{k_{x_\gamma}(\omega)\}|R^+_{\gamma,\nu}(\omega)|^2 \right) \tag{4a}$$

$$I_R(\omega) = \frac{\pi R}{\rho_0 \omega} \sum_{\nu} |A^+_\nu(\omega)|^2 \sum_{\mu} \left(\mathrm{Re}\{k_{x_\mu}(\omega)\}|T^+_{\mu,\nu}(\omega)|^2 \right) \tag{4b}$$

From the expressions of $I_L(\omega)$ and $I_R(\omega)$, we can define the incident $I^+_{inc}(\omega)$, reflected $I^+_{refl}(\omega)$ and transmitted $I^+_{transm}(\omega)$ acoustic intensities, as in Eq.s (5):

$$I^+_{inc}(\omega) = \frac{\pi R}{\rho_0 \omega} \sum_{\nu} \mathrm{Re}\{k_{x_\nu}(\omega)\}|A^+_\nu(\omega)|^2 \tag{5a}$$

$$I^+_{refl}(\omega) = \frac{\pi R}{\rho_0 \omega} \sum_{\nu} |A^+_\nu(\omega)|^2 \sum_{\gamma} \mathrm{Re}\{k_{x_\gamma}(\omega)\}|R^+_{\gamma,\nu}(\omega)|^2 \tag{5b}$$

$$I^+_{transm}(\omega) = \frac{\pi R}{\rho_0 \omega} \sum_{\nu} |A^+_\nu(\omega)|^2 \sum_{\mu} \mathrm{Re}\{k_{x_\mu}(\omega)\}|T^+_{\mu,\nu}(\omega)|^2. \tag{5c}$$

As we excite the system by one single mode ν at a time, we can define the intensity reflection $r^+_{I,\nu}$, transmission $t^+_{I,\nu}$ and absorption coefficient $\alpha^+_{I,\nu}$ relative to that single mode:

$$r^+_{I,\nu}(\omega) = \frac{\sum_\gamma \mathrm{Re}\{k_{x_\gamma}(\omega)\}|R^+_{\gamma,\nu}(\omega)|^2}{\mathrm{Re}\{k_{x_\nu}(\omega)\}} \tag{6a}$$

$$t^+_{I,\nu}(\omega) = \frac{\sum_\mu \mathrm{Re}\{k_{x_\mu}(\omega)\}|T^+_{\mu,\nu}(\omega)|^2}{\mathrm{Re}\{k_{x_\nu}(\omega)\}} \tag{6b}$$

$$\alpha^{+}_{I,\nu}(\omega) = 1 - |r_{I,\nu}(\omega)|^2 - |t_{I,\nu}(\omega)|^2, \tag{6c}$$

Analogously, the intensity scattering coefficients $r^{-}_{I,\sigma}(\omega)$, $t^{-}_{I,\sigma}(\omega)$ and $\alpha^{-}_{I,\sigma}(\omega)$ for each mode σ exciting the system from the right termination, can be retrieved after computing the scattering coefficients $R^{-}_{\mu,\sigma}(\omega)$ and $T^{-}_{\gamma,\sigma}(\omega)$.

After having defined the multi-modal scattering problem, we present now some interesting results concerning the attenuation of sound propagation achieved by both a purely local impedance boundary condition (BC), and the ABL. The ABL is an extension of the local BC, where the local impedance operator defines the relationship between the boundary acceleration and a Lagrangian (not Eulerian as for purely local BCs) derivative of sound pressure, with an advection speed given in the control. This boundary law is defined in [10, 5, 3, 4] and reported below:

$$Z_{Loc}(\partial_t) * \partial_t v_n = \partial_t p + U_b \partial_{arc\theta} p \quad \text{on } \partial\Omega. \tag{7}$$

In Eq. (7), $Z_{Loc}(\partial_t)$ is the differential operator in time domain corresponding to a local complex impedance, $*$ is the convolution operation, v_n is the velocity normal to the boundary $\partial\Omega$, p is the acoustic pressure, U_b is the advection speed and $arc\theta = R\theta$ is the arc relative to the angle θ and radius R. We define $M_b = U_b/c_0$. By defining the boundary advection along the azimuthal direction, we can contrast the propagation of the spinning modes, which are the most interested by rotating sources as turbofans.
We present here the simulation results obtained by such control law which has been also tested experimentally on the test-bench Phare2 [7, 8]. It is hence helpful for the interpretation and appreciation of the experimental results as well.
In Figure 3 we compare the scattering coefficients in case of purely local target impedance (ABL with $M_b = 0$), and advected law (ABL with $M_b = -2$), by exciting the first azimuthal modes with $m > 0$. Observe the enhancement of the transmission attenuation in case of $M_b = -2$, corresponding to an increase in the reflection coefficient. Note also that the mode with $m = 3$ cuts on around 950 Hz, and its transmission is significantly attenuated when $M_b = -2$. In Figure 4, we report the scattering coefficient by exciting the first azimuthal modes with $m < 0$, i.e. with the same sign as $M_b = -2$. Observe that the ABL with $M_b = -2$ shows a non-passive behaviour ($\alpha_I < 0$) when azimuthal modes rotating in the same sense as M_b.

These computations have very much helped to gain confidence about the expectable results in the experimental campaign. In addition, they can

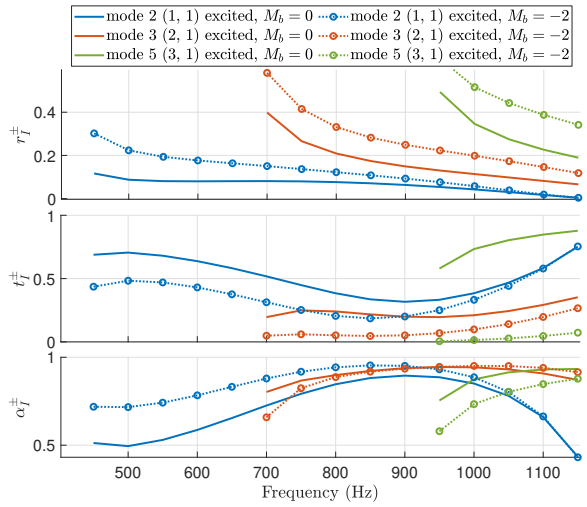

Figure 3: Intensity scattering coefficients in case of $M_b = 0$ and $M_b = -2$, for the first three modes with $m \neq 0$.

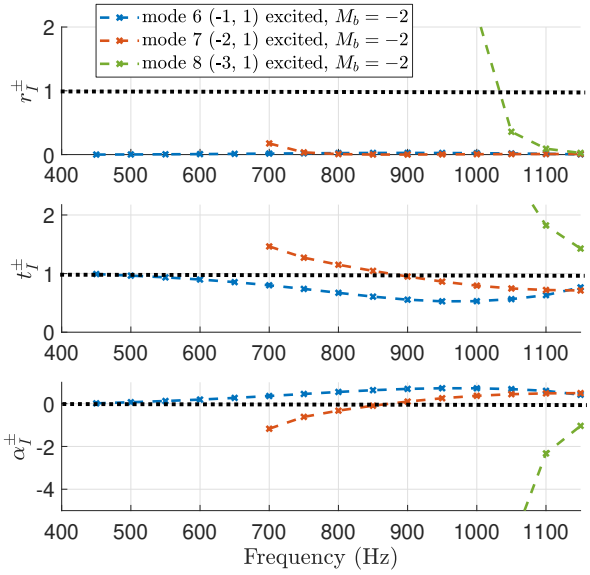

Figure 4: Intensity scattering coefficients in case of $M_b = 0$ and $M_b = -2$, for the first three modes with $m \neq 0$.

provide an useful tool for *optimization* of boundary control laws in multi-modal acoustic fields.

2 Experimental results

We wondered if such advection boundary control could be interesting for reducing noise radiation from a turbofan reproduction (scale 1 to 3), where the intake boundaries of the nacelle were treated by a circular electroacoustic liner, see Figure 5. In Figure 5, we also report the photo of the ER, the unit cell where the ABL is applied. Two rings of microphones are placed upstream and downstream the liner, in order to retrieve the azimuthal modal content of the sound field before and after the electroacoustic liner.

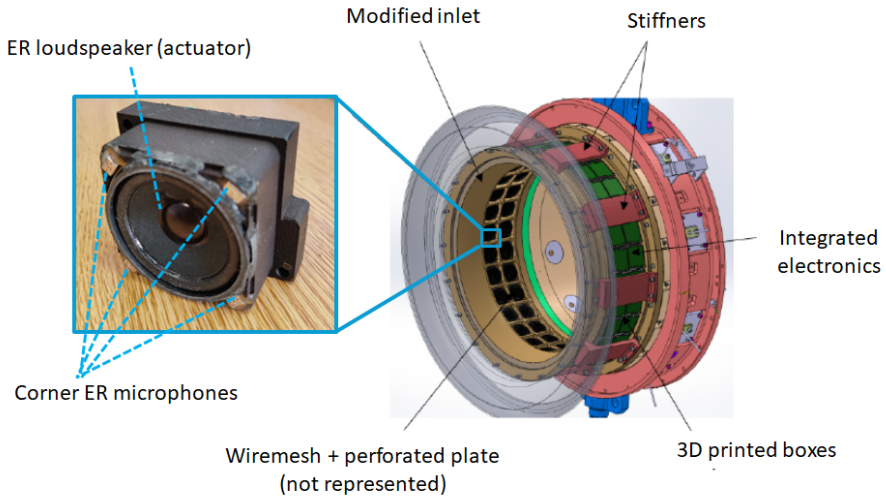

Figure 5: Photo of the single ER cell, and sketch of the modified inlet accommodating the electro-active liner.

In this case, the sound field is much more complex. But, due to the rotational speed of the turbofan, the predominant modes propagating in the nacelle are typically of spinning type. From that, the idea to adapt the advection boundary control, by imposing an advection speed along the azimuthal direction on the boundary, in opposite sense with respect to the rotational sense of the turbomachinery. Figure 7 shows what appeared in measurements: you see the average level of azimuthal modes around the Blade Passing Frequency (BPF), upstream and downstream the liner with respect to the airflow direction. Observe that here we are interested in reducing the radiation upstream the liner. Both measurements demonstrate that an $M_b = 2$ leads to an enhancement of the attenuation of mode $m = -3$, with respect to the case $M_b = 0$. Mode $m = -3$ is the most significant

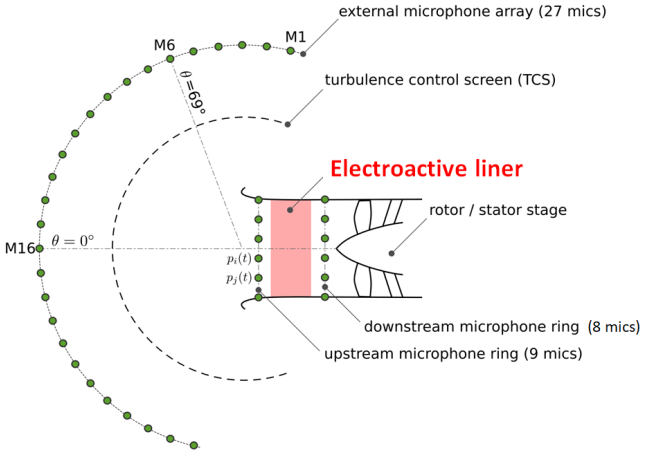

Figure 6: Sketch of the Phare2 duct stage.

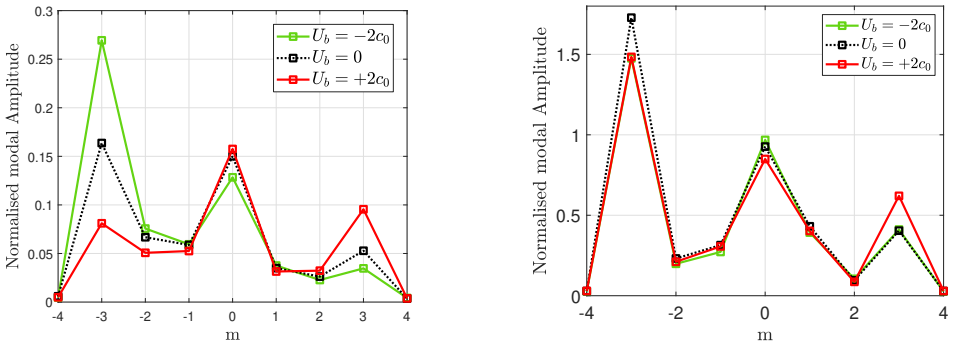

Figure 7: Normalized modal amplitude upstream (**a**) and downstream (**b**) the lined segment, around the Blade-Passing-Frequency (BPF) at 30% of the nominal engine speed, with varying U_b.

mode at this frequency, which is close to the cut-on frequency of mode $m = \pm 3$ as reported in the simulations of Section 1.1. Notice that introducing the advection speed M_b allows to improve attenuation of azimuthal modes having sign(m)= $-$sign(M_b), while modes with sign(m)=sign(M_b) are less attenuated, respect to the case $M_b = 0$. Notice also that the passivity issues found in the numerical simulations, are not featured in this experimental test bench. Remind that the simulations of Section 1.1 do not take into

account the airflow, and the presence of the wiremesh placed in front of the ERs.

3 Conclusions

We have presented an adaptation of the Advection Boundary Law to attenuate the spinning modes. Numerical simulations have allowed to gain confidence about the potentiality of such boundary control strategy. The multi-modal scattering simulation showed that the Advection Boundary Law can indeed attenuate the transmission of spinning modes rotating in the opposite sense as the boundary advection speed, though passivity issues can appear for the modes rotating in the same sense. The Phare2 experimental test-bench validated the numerical predictions in terms of attenuation of spinning modes, whereas no passivity issues have been featured. Nevertheless, the turbofan test-rig presents an aeroacoustic environment which is much more complex than the simulated one. Moreover, the electroacoustic liner synthesizing the Advection Boundary Law was covered by a wiremesh, which also contributes to increase the passivity margins.

ACKNOWLEDGMENTS

The SALUTE project has received funding from the Clean Sky 2 Joint Undertaking under the European Union's Horizon 2020 research and innovation programme under grant agreement N 821093. This publication reflects only the author's view and the JU is not responsible for any use that may be made of the information it contains.

References

[1] De Bono, E., Morell, M., Collet, M., Gourdon, E., Ture Savadkoohi, A., Ouisse, M., and Lamarque, C., "Model-inversion control to enforce tunable Duffing-like acoustical response on an Electroacoustic resonator at low excitation levels," *Journal of Sound and Vibration* **570**, 118070 (feb 2024).

[2] De Bono, E., Collet, M., Matten, G., Karkar, S., Lissek, H., Ouisse, M., Billon, K., Laurence, T., and Volery, M., "Effect of time delay on the impedance control of a pressure-based, current-driven Electroacoustic Absorber," *Journal of Sound and Vibration* , 117201 (2022).

[3] de Bono, E., Collet, M., Salze, E., Ouisse, M., Gillet, M., Lissek, H., Mardjono, J., Billon, K., and Volery, M., "Advection boundary law for sound transmission attenuation of place and spinning guided modes," in [*Forum Acusticum*], (2023).

[4] De Bono, E., Ouisse, M., Collet, M., Salze, E., and Mardjono, J., "A nonlocal boundary control, from plane waves to spinning modes control.," in [*Active and Passive Smart Structures and Integrated Systems XVII*], **12483**, 124831B, SPIE (2023).

[5] De Bono, E., *Electro-active boundary control for noise mitigation: local and advective strategies*, PhD thesis, Université de Lyon (2021).

[6] Salze, E., de Bono, E., Billon, K., Gillet, M., Volery, M., Collet, M., Ouisse, M., Lissek, H., and Mardjono, J., "Electro-active acoustic liner for the reduction of turbofan noise," in [*Forum Acusticum*], (2023).

[7] Salze, E., Pereira, A., Souchotte, P., Regnard, J., Gea-Aguilera, F., and Gruber, M., "New modular fan rig for advanced aeroacoustic tests-Acoustic characterization of the facility," in [*25th AIAA/CEAS Aeroacoustics Conference*], 2603 (2019).

[8] Pereira, A., Salze, E., Regnard, J., Gea-Aguilera, F., and Gruber, M., "New modular fan rig for advanced aeroacoustic tests-Modal decomposition on a 20" UHBR fan stage," in [*25th AIAA/CEAS Aeroacoustics Conference*], 2604 (2019).

[9] Rienstra, S. W., "Fundamentals of duct acoustics," *Von Karman Institute Lecture Notes* (2015).

[10] Karkar, S., De Bono, E., Collet, M., Matten, G., Ouisse, M., and Rivet, E., "Broadband Nonreciprocal Acoustic Propagation Using Programmable Boundary Conditions: From Analytical Modeling to Experimental Implementation," *Physical Review Applied* **12**, 054033 (nov 2019).